Energy Conversion and Management 83 (2014) 249–259

Contents lists available at ScienceDirect

Energy Conversion and Management

journal homepage: www.elsevier.com/locate/enconman

Hydrogen energy share improvement along with NO_x (oxides of nitrogen) emission reduction in a hydrogen dual-fuel compression ignition engine using water injection

V. Chintala *, K.A. Subramanian

Engines and Unconventional Fuels Laboratory, Centre for Energy Studies, IIT Delhi, New Delhi 110 016, India

ARTICLE INFO

Article history:
Received 2 January 2014
Accepted 29 March 2014
Available online 19 April 2014

Keywords:
Dual-fuel engine
Hydrogen
Specific water consumption
Energy share
NO_x emission

ABSTRACT

The study aims at enhancement of Hydrogen (H_2) energy share and reduction of Oxides of Nitrogen (NO_x) emission in a 7.4 kW-CI engine at 1500 rpm using water injection. The test engine was modified to run under dual-fuel operation with diesel–biodiesel blend (B20) and H_2 fuels for different Specific Water Consumption (SWC) of 130, 200, and 270 g/kWh. Under conventional H_2 dual-fuel mode, energy efficiency and NO_x emission increased significantly while Hydrocarbon (HC), Carbon Monoxide (CO) and smoke emissions decreased. The maximum H_2 energy share increased from 20% without water to 32%, 36%, and 39% with SWC of 130, 200, and 270 g/kWh respectively. However, SWC of 200 g/kWh was selected as an optimum water quantity for knock free operation, better performance and lower emissions. At the optimum SWC with 20% H_2 energy share, the NO_x emission and energy efficiency decreased about 24% and 5.7%, while HC and smoke emissions increased about 38% and 69%. At 20% H_2 energy share, the CO emission increased from 0.0 g/kWh without water to 1.2 g/kWh with the optimum SWC. However, reduction of these HC and CO emissions using oxidation catalysts needs to be studied further. A new methodology for determining heat release rate with consideration of crevice gas was proposed in the study.

1. Introduction

Hydrogen (H_2) could be the energy carrier of the future and excellent alternative fuel for internal combustion engines due to its favorable physiochemical properties. In India, it is envisaged in the National Hydrogen Energy Roadmap by Ministry of New and Renewable Energy that one million H_2 fueled vehicles and decentralized H_2 based power generation of about 1000 MW aggregate capacity would be targeted in the country by 2020 [1]. On the other hand, biodiesel could be a clean and renewable fuel as it has no carcinogens, less sulfur content and has the potential to be an alternate for Petro-diesel fuel in the long run. In India, as the diesel consumption is about 5 times higher than gasoline consumption [2], simultaneous utilization of H_2 and biodiesel in Compression Ignition (CI) engines under dual-fuel mode would enhance sustainability of the diesel driven economy. Dual-fuel technology offers a major advantage of fuel flexibility that the engine could run either in a neat diesel mode with 100% diesel fuel or in dual-fuel mode whenever gaseous fuel is available [2]. In addition to those inferior quality gaseous fuels having lower heating values including biogas could also be utilized in a CI engine without major hardware modifications under dual-fuel strategy. For instance, Bedoya et al. used biogas in a CI engine of rated power 60 kW at 3300 rpm under homogeneous charge compression ignition mode with equivalence ratios of 0.25–0.4 [3]. Swami Nathan et al. found 50% biogas energy share as the optimum value for better performance and lower emissions with homogeneous charge operation in a 3.5 kW-CI engine at 1500 rpm [4]. The maximum diesel substitution with biogas was achieved about 49% in a single cylinder indirect injection CI engine at rated load and speed of 7.73 kW and 1800 rpm [5]. Makareviciene et al. utilized maximum amount of biogas about 40 liters per minute along with diesel fuel in a 60 kW multi cylinder turbocharged direct injection CI engine [6].

Other than biogas as a fuel in CI engines, natural gas and H_2 have also been utilized as fuels by some investigators. With the utilization of natural gas as main fuel and diesel as pilot fuel under dual-fuel operation, Oxides of Nitrogen (NO_x) emission decreased significantly [7]. Saravanan inducted the H_2 into the intake manifold along with the conventional direct diesel injection into the cylinder [8]. Such an operation resulted in an increase of energy efficiency, reduction in Hydro Carbon (HC), Carbon Monoxide

* Corresponding author. Tel.: +91 11 26591247 (O), mobile: +91 8595071337; fax: +91 011 26581121.
E-mail address: venkatchintala12@gmail.com (V. Chintala).

http://dx.doi.org/10.1016/j.enconman.2014.03.075
0196-8904/

Nomenclature

$\frac{\partial q}{\partial x_1}, \frac{\partial q}{\partial x_2}, \ldots \frac{\partial q}{\partial x_n}$	partial differential of calculated parameter q which depends on different measured variables $x_1, x_2, \ldots, x_n$
$\dot{R}$	universal gas constant (J/mol K)
$\dot{m}$	mass flow rate of fluid/species (kg/s)
$[N_2]$, [NO], $[H_2O]$, $[O_2]$	nitrogen, nitric oxide, water, and oxygen concentrations (mol/cm^3)
[O], [OH]	oxygen and hydroxyl radical concentrations (mol/cm^3)
A	area of cylinder (m^2)
ABDC	after bottom dead center
ATDC	after top dead center
B	cylinder bore (m)
B20	diesel (80% volume) biodiesel (20% volume) blend
BBDC	before bottom dead center
B_c	clearance between piston and cylinder liner (m)
BDC	bottom dead center
BP	brake power (kW)
BTDC	before top dead center
C	carbon atom
CA	crank angle (degrees)
ch	charge
CI	compression ignition
CO	carbon monoxide
CO_2	carbon dioxide
COV	coefficient of variation (%)
C_p	specific heat at constant pressure (kJ/kg K)
cr	crevice
C_v	specific heat at constant volume (kJ/kg K)
CV	calorific value (kJ/kg)
d(NO)/dt	mass reaction rate of NO (gm/cycle)
d[NO]/dt	molar reaction rate of NO (mol/cm^3 s)
d_α, d_1, d_2, d_3, d_4, d_5	constants
EOI	end of injection
EVC	exhaust valve closing
EVO	exhaust valve opening
H	hydrogen atom/radical
H_2	hydrogen gas
H_2O	water
h_c	convective heat transfer coefficient (kW/m^2 K)
HC	hydrocarbon emission
h_{tl}	crevice top land height (m)
IMEP	indicated mean effective pressure (N/m^2)
IVC	inlet valve closing
IVO	inlet valve opening
$k_{b,11}$, $k_{b,12}$, $k_{b,13}$	backward reaction rate constants (cm^3/mol s)
$k_{f,11}$, $k_{f,12}$, $k_{f,13}$, $k_{f,\mathrm{CO}}$	forward reaction rate constants (cm^3/mol s)
lh	latent heat
MW	molecular weight
N	nitrogen atom
N_2	nitrogen
NO	nitric oxide (g/kWh)
n_{O2}	number of moles of oxygen
NO_x	Oxides of Nitrogen (g/kWh)
n_{TP}	total number of moles of products
Ø	equivalence ratio
O	oxygen atom
O_2	oxygen
OH	hydroxyl radical
p	in-cylinder pressure (N/m^2)
q	calculated parameter
Q	heat energy/heat transfer/heat release (kW)
R	hydrocarbon radical
S	engine speed (rpm)
sat	saturation
sh	sensible heat
SOI	start of injection (°CA)
suh	superheat
SWC	specific water consumption (g/kWh)
T	temperature (K)
TDC	top dead center
U	internal energy (kW)
V	cylinder instantaneous volume (m^3)
V_{cr}	crevice volume (m^3)
v_{gas}	velocity of gases inside the cylinder (m/s)
vp	vapor
W	work energy (kW)
wa	walls of cylinder
WFR	water fuel ratio
wtr	water
x	mole fraction
$x_1, x_2, \ldots x_n$	measured variables
α	molar ratio of fuel to air
β	molar ratio of fuels
γ	specific heat ratio
ε, ε_0, ω	auxiliary quantities for specific enthalpy (J/kg)
ζ	molar ratio of water to fuel
ρ	density of species/fluid (kg/m^3)
θ	degree crank angle

(CO), Carbon Dioxide (CO_2) and volumetric efficiency. With the addition of H_2 into the CI engine, NO_x emission increased and smoke decreased substantially [9]. As H_2 being carbon free energy carrier, it decreased CO_2 emission due to reduction in total carbon content in the diesel-H_2 mixture and smoke emission due to improvement in degree of homogeneity in the premixed charge [10]. Even though all carbon based emissions, including smoke/soot decrease with the addition of H_2 into the CI engine, higher NO_x emission will be a major challenge resulting in difficult to implement it in the dual-fuel engine systems. Moreover, higher amounts of H_2 cannot be utilized in conventional dual-fuel engines due to knocking problem. Abnormal rate of pressure rise due to combustion is generally considered as knocking. Selim reported that the increasing mass of gaseous fuel (liquefied petroleum gas/methane/natural gas) lead to significant increase in the maximum rate of pressure rise in a single cylinder variable compression indirect injection diesel engine (Ricardo E6: 9 kW rated power) [11]. He also concluded that the gaseous fuel existing in the combustion chamber could be more susceptible to auto-ignite with increasing in-cylinder temperature. To address these issues, various strategies such as exhaust gas recirculation, ignition timing retardation, and the addition of diluents including nitrogen, CO_2, and water are available among which water injection technique could be the viable option.

Water injection is the most effective means for solving the twin problem of high NO_x emission and low H_2 energy share with the additional benefit of knock and backfire free operation because the water cools the thermal sources of ignition and alters chemical reaction rate. The capability of water to absorb the heat of combustion, specifically at high temperature range reduces the temperature of combustion products and leads to lower NO_x emission. Carlucci et al. developed a closed loop low temperature combustion control mechanism for reduction of NO_x emission in a CI engine [12]. Nande et al. reported 55% NO_x reduction with the water injection into the intake manifold of a H_2 fueled direct injection spark ignition engine at a marginal

loss of energy efficiency [13]. Palash et al. reviewed on NO_x emission mitigation technique of water injection and found the emission reduction about 10–38% from CI engines [14]. Prabhukumar et al. inducted water along with the intake charge of a H_2 dual-fuel engine. Induction of water into the intake manifold along with H_2 increased the knock limited power output as it serves as the powerful internal coolant in decreasing the unburned mixture temperature [15]. Boretti also reported the reduction in combustion temperature and knocking tendency with water injection in multi cylinder spark ignition engine [16]. Some researchers worked on a small capacity CI engine Gen-set system under H_2 dual-fuel mode using diluents such as helium, nitrogen and water [17]. They found that H_2 could be substituted for diesel fuel up to 38% of full-load energy with no penalty of efficiency and power output. Nevertheless, they succeeded up to 66% H_2 energy substitution along with water injection. Subramanian reported the decreased Nitric Oxide (NO) emission from 1034 ppm with base diesel to 643 ppm with water injection at full load operation in a direct injection diesel engine [18]. Tauzia et al. investigated the effect of water as liquid and vapor injection on ignition delay, rate of heat release and emission of an automotive turbocharged direct injection CI engine [19]. They utilized the water mass of about 60–65% of the fuel and succeeded 50% NO_x reduction. Tesfa et al. utilized manifold water injection system to reduce the problem of high NO_x emission from biodiesel fueled diesel engine [20]. It was reported that water injection of 3 kg/h resulted in NO_x reduction by 50% without deteriorating engine performance due to reduction in premixed combustion temperature. However, HC, CO and smoke emissions increased with increase in water content with intake air [21]. Adnan et al. conducted experiments on a port injected H_2 dual-fuel engine with varying water injection timings from 20° Before Top Dead Centre (BTDC) to 20° After Top Dead Centre (ATDC) in steps of 10° Crank Angle (CA) for two different injection durations of 20° and 40° CA [22]. Better performance due to increased gross indicated work and indicated thermal efficiency was observed with the water injection timing of 20° ATDC and duration of 20° CA.

Some investigations have been reported on NO_x emission reduction from CI engines using water emulsions. For instance, Alahmer reported the NO_x emission reduction from 500 ppm with the base diesel operation to 112 ppm with 30% water emulsion in multi cylinder direct injection diesel engine at 1550 rpm [23]. He also reported the emission reduction about 45% with 30% water content by volume at 3000 rpm [24]. Combustion of emulsified fuel decreased the NO_x emission due to the finely dispersed water droplets of the emulsion act as a heat sink which reduces the localized in-cylinder temperature. Substantial reduction in both NO_x and particulate matter emissions was achieved with combined use of water emulsion and oxygen enrichment of intake air from a CI engine [25]. The presence of water in the emulsion and its micro-explosion phenomenon decreased the NO_x emission. Debnath et al. reported the emission reduction about 20% with water emulsified biodiesel fuel from a 3.5 kW single cylinder CI engine at 1500 rpm [26]. Some investigations have been reported on steam injection into CI engines for NO_x emission reduction. Gonca reported about 34% reduction in NO emission with supply of the optimum steam rate i.e., 20% of injected fuel by mass in a 13 kW direct injection diesel engine [27]. Cesur et al. reported about 40% reduction in NO_x emission with steam injection in a spark ignition engine [28].

From the literature survey, it is emerged that water addition into a CI engine either in direct liquid or emulsion or steam form could decrease the NO_x emission drastically due to occurrence of low temperature combustion. This strategy in H_2 dual-fuel operation enhances the knock limited H_2 energy share. In the present study, timed manifold water injection technique has been adopted in order to address the twin problem of high NO_x emission and low percentage of H_2 substitution in a H_2 dual-fuel engine. Water induction could also reduce the occurrence of backfiring and knocking tendency in dual-fuel engines.

2. Experimental methodology

2.1. Experimental setup

An experimental setup was developed to conduct tests as shown in Fig. 1. It consists of a four stroke naturally aspirated diesel engine coupled with an eddy current dynamometer for engine loading, an intake air system for measurement of volumetric air flow rate, an electronic weighing balance for measurement of liquid fuel consumption, an exhaust gas emission analyzer for measuring CO and HC emissions, a Smoke meter for smoke measurement, and a Chemiluminescense analyzer for NO_x measurement. The test engine main specifications are given in Table 1. The engine was converted for dual-fuel operation. A timed manifold injection system was developed for injecting H_2 gaseous fuel into the intake manifold as shown in Fig. 1. It consists of an electronic control unit (ECU), solenoid gas injector, gas mass flow meter, high and low pressure fuel lines, and pressure gauge. The same injection system was also used for injecting water with a solenoid liquid injector into the intake manifold. The ECU controls both H_2 and water injection timings i.e., Start of Injection (SOI) and End of Injection (EOI) for different loads. Water and H_2 were injected into the intake manifold at 2 bar and 3 bar respectively, while Diesel–Biodiesel blend (B20: Diesel 80% volume and Karanja Biodiesel 20% volume) was directly injected into the cylinder at 250 bar using a conventional liquid injector. A piezoelectric pressure transducer with nominal sensitivity 45 picocoulomb/bar was mounted on the cylinder head of the engine for in-cylinder pressure measurement. An optical encoder was mounted on the engine's crankshaft for crank angle measurement with an accuracy of 0.1°CA. The in-cylinder pressure analog signal was amplified by the charge amplifier and then, the analog signal was converted to a digital signal from the data acquisition system for further processing of the acquired data. The post processing software named AVL Indicom Light was used for processing of pressure-crank angle data. In-cylinder temperatures are calculated using ideal gas equation with the input of in-cylinder pressure data. Physio-chemical properties of fuels used in the experiments are given Table 2.

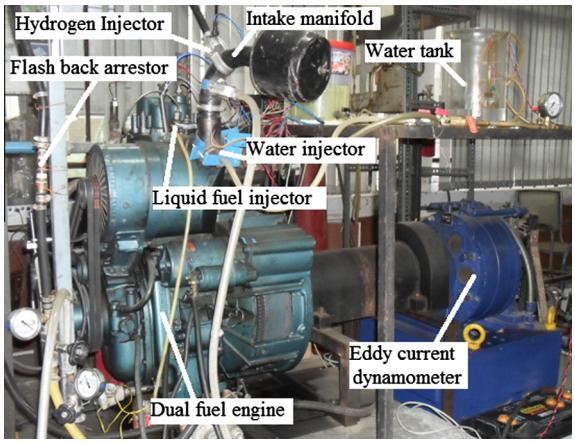

Fig. 1. Photographic view of the experimental setup.

Table 1
Technical specifications of the engine.

S. No.	Parameter	Description
1	Make and model	Kirloskar and EA10
2	Number of cylinders	1
3	Displacement volume, cc	947.4
4	Rated power output, kW	7.4
5	Rated speed, rpm	1500
6	Bore × stroke, mm	102 × 116
7	Compression ratio	19.5:1
8	Connecting rod length, mm	232.6
9	Intake valve opening and closing, degree crank angle	43 BTDC and 67 ABDC
10	Exhaust valve opening and closing, degree crank angle	87 BBDC and 39 ATDC

Table 2
Properties of fuels used.

S. No.	Fuel characteristics	Diesel biodiesel blend (B20)	Hydrogen
1	Molecular structure	$C_{14.1}H_{29.6}O_{0.15}$	H_2
2	Lower heating value, MJ/kg	42.6	120
3	Stiochiometric air fuel ratio	13.8	34.2
4	Auto ignition temperature, K	–	858
5	Laminar burning velocity, m/s	–	2.65–3.25
6	Cetane number	50.3	–
7	Density, kg/m^3	835.6	0.083
8	Viscosity, cSt	2.71	–

2.2. Experimental procedure

Experimental tests were carried out with B20 as pilot fuel for initiating the ignition and H_2 as main fuel for Specific Water Consumption (SWC) of 130, 200, and 270 g/kWh at 100% load and a constant speed of 1500 rpm. The SWC is determined using Eq. (1) and the calculation for a particular energy share is shown in Appendix A. Water and H_2 were injected into the intake manifold during the suction stroke while B20 was directly injected into the cylinder at the end of compression stroke. Valve timing diagram including start and end of H_2/water injection is shown in Fig. 2. The SOI for H_2 and water kept constant as 43° and 45° CA-ATDC throughout the experiments in order to avoid scavenging losses during valve overlapping period. The EOI for both fluids (H_2 and water) varied independently with respect to H_2 energy share and water consumption. Based on the maximum available time for reaching the injected gas from the point of injection in the intake manifold to the engine cylinder, the duration of injection was optimized in the earlier study [29]. The same methodology was applied for water injection in the present study. With the maximum allowable injection time, the SWC could achieve as 270 g/kWh. If it continues beyond this quantity, the injected water could accumulate in the intake manifold. The accumulation of water in the manifold steered up the corrosion and durability problems. Hence, the SWC 270 g/kWh was fixed as the maximum water quantity that could be injected via intake manifold. The remaining quantities of injected water, i.e., 130 and 200 g/kWh were selected arbitrarily for the study. For a particular SWC, the H_2 energy share was increased to a maximum limit of in-cylinder peak pressure and maximum rate of pressure rise. The details pertaining to the maximum percentage of H_2 substitution with reference to different SWCs will be discussed in the Section 4.2.

Prior to the test engine running, analyzers were calibrated as per the manufacturer's recommended procedure. Initially, the sample gas flow lines were purged with nitrogen (N_2) gas and

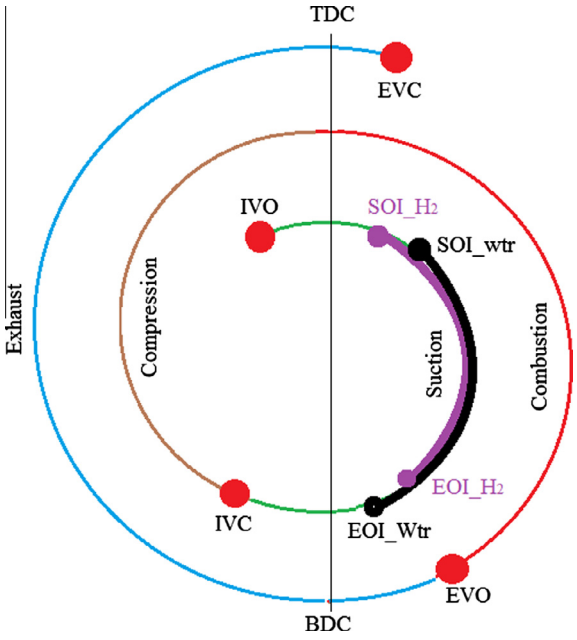

Fig. 2. Valve timing diagram with injection timing of H_2/Water.

subsequently made zero calibration of all independent measuring parameters using the same gas. Then dynamic calibration was carried out with different span gases of known measurement values. For example, NO gas used for Chemiluminescense analyzer, and CO, CO_2 and hexane were used for the Di-gas analyzer. The measurement range and its accuracy for different parameters are given in Table 3. All experimental measurements, irrespective of the type of instrument used, possess some uncertainty. Uncertainties of various parameters are determined using Eq. (2) [29] and their values are given in Table 3.

$$\mathrm{SWC} = \frac{3600\dot{m}_{wtr}}{BP} \times 1000 \tag{1}$$

$$q = \left[\left(\frac{\partial q}{\partial x_1}\Delta x_1\right)^2 + \left(\frac{\partial q}{\partial x_2}\Delta x_2\right)^2 + \ldots\ldots\ldots + \left(\frac{\partial q}{\partial x_n}\Delta x_n\right)^2\right]^{\frac{1}{2}} \tag{2}$$

Table 3
Accuracies of measurements and uncertainties.

S. No.	Parameter	Measuring range	Accuracy	Uncertainty (%)
1	NO_x emission	<1000 ppm volume ⩾ 1000 ppm volume	±5 ppm ± 5% of value	2.692
2	HC emission	<2000 ppm volume ⩾ 2000 ppm volume	±10 ppm ± 4% of value	3.09
3	CO emission	<0.7% volume ⩾0.7% volume	±0.03% ±3% of value	3.92
4	Smoke emission	0–100% opacity	±1% of value	2.512
5	Volume flow rate of air	0–500 m^3/h	±2% of flow	1.7
6	Mass flow rate of hydrogen	0–5 kg/h	±1% of flow	1.4
7	Brake power	–	–	0.197
8	Energy efficiency	–	–	0.25
9	Mass flow rate of B20	–	–	2.3
10	Heat transfer loss	–	–	2.432

3. Proposed theoretical model for heat release rate and NO_x formation

3.1. Heat release rate with consideration of crevice volume

In conventional single fuel i.e., diesel operation, only air enters into the combustion chamber during the suction stroke subsequently it is pushed into the crevices during compression while in case of H_2 dual-fuel operation, air–fuel mixture (H_2 + air) enters into the chamber during suction stroke. During compression and early part of the combustion process, this air–fuel charge is pushed into the crevice volumes which causes considerable amount of heat losses as the charge remains in the crevice volume during the combustion. In order to account these heat losses, a new methodology for calculating heat release rate during combustion in the H_2 dual-fuel engine using the first law of thermodynamics with consideration of crevice effects (Eqs. (3)–(10)) is proposed in the study. Since crevice effects are comparatively small, an accurate model for their overall effect is to consider a single aggregate volume (top land crevice volume; V_{cr}) where the gas pressure is almost equal to the pressure in the combustion chamber, but at a different temperature. In the present study, it is assumed that the temperature of crevice gas equals to cylinder wall temperature. Woshchni correlation can be used for calculating heat transfer coefficient as given in Eq. (8) [30].

$$\delta Q = dU + \delta W + \delta Q_{wa} + \delta Q_{cr} \tag{3}$$

where

$$dU = \dot{m}_{ch} C_v(T) dT \tag{4}$$

$$\delta W = pdV \tag{5}$$

$$\delta Q_{wa} = h_c A (T - T_{wa}) \tag{6}$$

$$\delta Q_{cr} = \dot{m}_{cr} C_p(T) dT \tag{7}$$

$$h_c = 0.82 B^{-0.2} p^{0.8} v_{ch}^{0.8} T^{-0.53} \tag{8}$$

With the use of ideal gas equation, the Eq. (3) could be rearranged with respect to degree crank angle as given in Eq. (9).

$$\frac{dQ}{d\theta} = \frac{\gamma}{\gamma - 1} p \frac{dV}{d\theta} + \frac{1}{\gamma - 1} V \frac{dp}{d\theta} + h_c A \frac{dT_{wa}}{d\theta} + \frac{\gamma}{\gamma - 1} V_{cr} \frac{dp}{d\theta} \tag{9}$$

where

$$V_{cr} = \Pi B B_c h_{tl} \tag{10}$$

3.2. NO_x formation in dual-fuel engines

In the present study, extended Zeldovich mechanism (Eqs. (11)–(13)) is used for theoretical modeling of NO formation in the CI engine with B20 as pilot fuel and H_2 as the main fuel under dual-fuel operation [30].

$$O + N_2 \quad k_{f,11} \leftrightarrow k_{b,11} \quad NO + N \tag{11}$$

$$NO + N \quad k_{f,12} \leftrightarrow k_{b,12} \quad O + N_2 \tag{12}$$

$$N + O_2 \quad k_{f,13} \leftrightarrow k_{b,13} \quad NO + N \tag{13}$$

where

$$k_{f,11} = (1.8 \times 10^{14}) \exp(-38,370/T) \tag{14}$$

$$K_{b,11} = (3.8 \times 10^{13}) \exp(-425/T) \tag{15}$$

$$K_{f,12} = (1.8 \times 10^{10}) T \exp(-4680/T) \tag{16}$$

$$K_{b,12} = (3.8 \times 10^{9}) T \exp(-20,820/T) \tag{17}$$

$$K_{f,13} = (7.1 \times 10^{13}) \exp(-450/T) \tag{18}$$

$$K_{b,13} = (1.7 \times 10^{14}) \exp(-24,560/T) \tag{19}$$

The combustion reaction in a CI engine under conventional dual-fuel mode with H_2 as main fuel and B20 pilot fuel is given in Eq. (20).

$$\alpha(C_{14.1}H_{29.6}O_{0.15} + \beta H_2) + (n_{O2}/\emptyset)(O_2 + 3.76N_2) \rightarrow n_{TP}(x_{CO2}CO_2 + x_{H2O}H_2O + x_{N2}N_2 + x_{O2}O_2 + x_{H2}H_2 + x_{CO}CO) \tag{20}$$

With addition of water in the dual-fuel engine, the practical combustion reaction could be written as Eq. (21). The NO formation rate could be determined theoretically using Eq. (26). Mass emission formation of NO is given by Eqs. (31) and (32).

$$\alpha(C_{14.1}H_{29.6}O_{0.15} + \beta H_2 + (\zeta/\emptyset)H_2O) + (n_{O2}/\emptyset)(O_2 + 3.76N_2) \rightarrow n_{TP}(x_{CO2}CO_2 + x_{H2O}H_2O + x_{N2}N_2 + x_{O2}O_2 + x_{H2}H_2 + x_{CO}CO) \tag{21}$$

where

$$\propto = \frac{0.21}{14.1 + \left(\frac{29.6+2\beta}{4}\right) - \left(\frac{0.15}{2}\right)} \tag{22}$$

$$\beta = \frac{(\dot{m}_{H2} MW_{B20})}{(\dot{m}_{B20} MW_{H2})} \tag{23}$$

$$\zeta = (WFR(MW_{B20} + MW_{H2}))/MW_{H2O} \tag{24}$$

$$WFR = \frac{\dot{m}_{wtr}}{(\dot{m}_{B20} + \dot{m}_{H2})} \tag{25}$$

$$\frac{d[NO]}{dt} = \frac{2k_{f,15}[O][N_2]\left(1 - \frac{k_{b,15}k_{b,16}[NO]^2}{k_{f,15}k_{f,16}[N_2][O_2]}\right)}{1 + \frac{k_{b,15}[NO]}{k_{f,16}[O_2] + k_{f,17}[OH]}} \tag{26}$$

Nitrogen [N_2], oxygen [O_2], and oxygen [O] and hydroxyl [OH] radical concentrations are determined using Eqs. (27)–(30).

$$[N_2] = \frac{p}{\dot{R}T} x_{N2} \tag{27}$$

$$[O_2] = \frac{p}{\dot{R}T} x_{O2} \tag{28}$$

$$[O] = 0.397 T^{-0.5} [O_2]^{0.5} \exp(-31090/T) \tag{29}$$

$$[OH] = 2.13 \times 10^{-4} T^{-0.6} [O][H_2O]^{0.5} \exp(-4595/T) \tag{30}$$

$$\frac{d(NO)}{dt} = \frac{d[NO]}{dt} \frac{(MW_{NO})\dot{R}TS}{120p} \tag{31}$$

$$\text{NO in mass emission} = \frac{d(NO)}{dt} \frac{30S}{BP} \tag{32}$$

4. Results and discussion

4.1. Effect of water injection on energy efficiency

Fig. 3 shows a significant increase in energy efficiency with increasing H_2 energy share in H_2 dual-fuel engine at 100% load

and 1500 rpm. Energy efficiency and H_2 energy share could be determined using Eqs. (33) and (34) and the specific calculations for a particular energy share are given in Appendix A. Energy efficiency increased from 30.8% with base B20 fuel to 35% with 20% H_2 energy share. The reasons for the increase in the efficiency are better mixing of fuel with air due to the higher diffusivity of H_2 (0.63 cm^2/s) and the higher peak pressure/temperature as compared to the base B20 mode i.e., 0% H_2 energy share (Fig. 4(a)). In-cylinder pressure and temperature profiles with respect to degree CA are shown in Fig. 4. As H_2 have high heat content and burning velocity, the pressure/temperature increased significantly. Due to rapid combustion, the ignition delay and combustion duration decreased with increasing H_2 energy share as shown in Fig. 5(a). The decreasing trend in combustion duration indicates the occurrence of constant volume combustion, which directly promotes the energy efficiency significantly. In the previous investigations, the increase in energy efficiency about 10% with 18% H_2 energy share under dual-fuel operation due to reduction in combustion irreversibility in a direct injection diesel engine was reported [31]. They also reported the H_2 utilization in the diesel engine enhanced the degree of constant volume combustion due to its high flame velocity, which resulted in high combustion and energy efficiency [32]. Heat release rate traces with respect to degree CA are depicted in Fig. 6. The heat release rate traces for the H_2 dual-fuel operation are determined with consideration of a crevice gas mixture of H_2 and air as discussed in the Section 3.1. The cumulative heat release rate increased correspondingly with increasing combustion temperature. However, for a particular H_2 energy share, the efficiency decreased with increasing SWC as shown in Fig. 3. For example, at 20% H_2 energy share, efficiency decreased from 35% without water to 34%, 33.1%, and 31.9% with SWC of 130, 200, and 270 g/kWh respectively because of reduced in-cylinder temperature and the cumulative heat release rate. In the present study, as the knock limited H_2 energy share with the conventional H_2 dual-fuel operation was 20%, the same percentage is used as a reference point for comparing all other results with water added H_2 dual-fuel operation. Prabhukumar et al. reported the similar decreasing trend in thermal efficiency from 19% without water to 15% and 9% with water consumption of 0.4×10^{-3} and 0.7×10^{-3} m^3/h in a H_2 dual-fuel engine [15].

$$\text{Energy efficiency} = \frac{BP}{(\dot{m}_{H2} \times CV_{H2}) + (\dot{m}_{B20} \times CV_{B20})} \times 100 \quad (33)$$

$$\text{Hydrogen energy share} = \frac{\dot{m}_{H2} \times CV_{B20}}{(\dot{m}_{H2} \times CV_{H2}) + (\dot{m}_{B20} \times CV_{B20})} \times 100 \quad (34)$$

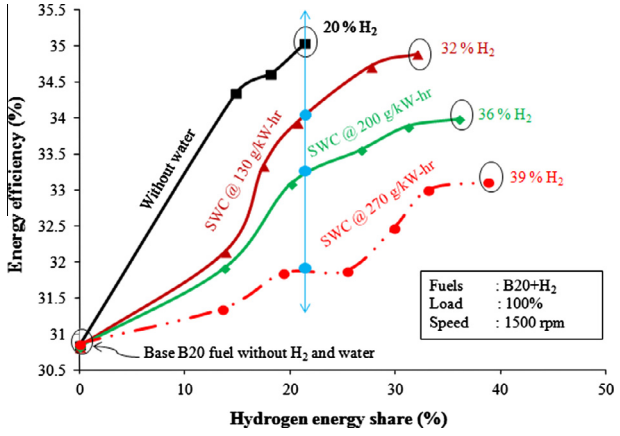

Fig. 3. Energy efficiency verses H_2 energy share.

4.2. Effect of water injection on energy share

Hydrogen energy share increases drastically with an increase in injected water quantity as shown in Fig. 3. It increased from 20% without water injection to 32%, 36%, and 39% with SWC of 130, 200, and 270 g/kWh respectively. The in-cylinder peak pressure values with 32%, 36%, and 39% H_2 energy shares were 89.01, 88.16, 88.64 bar respectively at 100% load and 1500 rpm. The pressure profile for 36% H_2 energy share is shown in Fig. 4(a). Beyond these percentage of H_2 energy shares, the peak pressure values were shooting above 90 bar. As the permissible in-cylinder peak pressure by the engine manufacturer is 90 bar for full load operation, these H_2 energy shares i.e., 32%, 36%, and 39% were considered as the maximum energy shares that could be substituted under dual-fuel operation with SWC of 130%, 200%, and 270 g/kWh. Prabhukumar et al. also reported an increase in knock limited power output about 19% and 39% with water addition of 0.4×10^{-3} and 0.7×10^{-3} m^3/h respectively in a H_2 dual-fuel engine [15]. Water in the combustion chamber absorbs the heat which is generated during combustion of fuel. This total heat absorption is typically classified into three types; sensible heat, latent heat, and superheat. Heat absorption rates are determined using Eqs. (35)–(38) [33]. Fig. 7 shows the contribution of three distinct types of heat energy absorbed by the water in the cylinder. It is clearly seen from the figure that the amount of heat absorbed by water inside the combustion chamber increased significantly with increasing quantity of water. It increased from 158.7 J/cycle with SWC of 130 g/kWh to 326.9 J/cycle with SWC of 270 g/kWh.

$$\text{Sensible heat, } Q_{sh} = \dot{m}_{wtr}\left[\in + \left(\frac{T}{\rho_{wtr}}\frac{dp}{dT_{wtr}}\right)\right] \quad (35)$$

$$\text{Latent heat, } Q_{lh} = \dot{m}_{wtr}\left[\varepsilon + \left(\frac{T}{\rho_{vp}}\frac{dp}{dT_{vp}}\right)\right] \quad (36)$$

$$\text{Superheat, } Q_{\text{suh}} = \dot{m}_{wtr}\left[Q_{\text{lh}} + C_{p,\text{suh}}(T_{\text{suh}} - T_{\text{sat}})\right] \quad (37)$$

$$\frac{\varepsilon}{\varepsilon_0} = d_\propto + d_1\omega^{-19} + d_2\omega + d_3\omega^{4.5} + d_4\omega^5 + d_5\omega^{54.5} \quad (38)$$

where $\varepsilon_0 = 1000$ J/kg, $d\alpha = -1135.906$, $d_1 = -5.651 \times 10{-}8$, $d_2 = 2690.666$, $d_3 = 127.287$, $d_4 = -135.003$, and $d_5 = 0.982$.

As the in-cylinder temperature is higher than the saturation temperature of water inside the combustion chamber at a particular in-cylinder pressure, the entire amount of injected water could convert to superheated steam. From Fig. 7 it is clearly seen that heat absorbed for superheating of water is higher than the other two types of heat energy. It is observed that superheat contributes about 63% of the total heat absorbed by the water. A notable point is emerged from this study that degree of superheat contributes a major share towards temperature reduction of the charge with supply of water. The cumulative heat release rate for 20% H_2 energy share decreased from 1866.4 J/cycle with conventional dual-fuel mode to 1798.8 J/cycle with water added dual-fuel mode at the SWC of 200 g/kWh. In-cylinder peak temperature increased significantly with increasing H_2 energy share, but it decreased extensively with increasing quantity of water as shown in Fig. 8. At 20% H_2 energy share, peak temperature decreased from 1965 K without water injection to 1939, 1893, and 1865 K with SWC of 130, 200, and 270 g/kWh respectively (Fig. 8). This reduction in temperature helps to enhance the H_2 energy share significantly under dual-fuel operation. It may be noted that the maximum H_2 energy share and the amount of water added in the H_2 dual-fuel engine is limited by various parameters including peak in-cylinder pressure, maximum rate of pressure rise, and Coefficient of Variation in Indicated Mean Effective Pressure

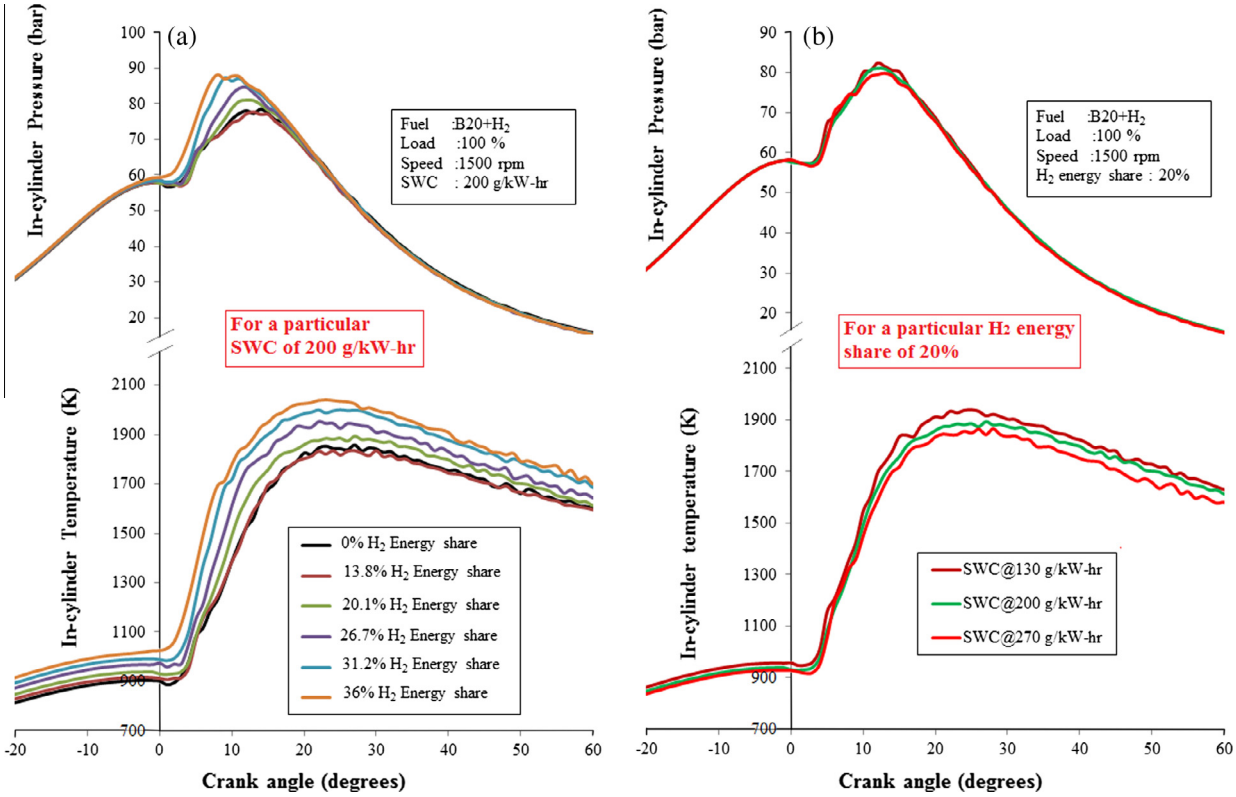

Fig. 4. In-cylinder pressure and temperature profiles with respect to degree CA.

(COV_{IMEP}). From Figs. 8 and 9, it could be inferred that the addition of water up to 200 g/kWh would give beneficial results beyond which both maximum rate of pressure rise and COV in IMEP increase abruptly. Water to Fuel Ratio (WFR) increased with increasing H_2 energy share as shown in Fig. 9. In the present study, the ratio reaches up to 1 with water addition of 200 g/kWh and 36% H_2 energy share under dual-fuel mode. Subramanian also injected water in a direct injection diesel engine of 4.5 kW at 1500 rpm with the ratio of 0.4 and stated that higher NO reduction could be achieved with higher ratios [18]. With 200 g/kWh water supply, energy efficiency (34%) is almost comparable with conventional dual-fuel engine without water supply (35%) as seen in Fig. 3. A significant reduction in NO_x emission was observed for the same operating conditions which will be discussed in the Section 4.3. Similarly, slight increase in carbon based emissions (HC, CO and smoke) could be observed with the water supply of 200 g/kWh which will be discussed in Section 4.4. With these inferences, water addition of 200 g/kWh to the H_2 dual-fuel engine is selected as an optimum water quantity for better performance and lower emissions at rated load and speed.

4.3. Effect of water injection on NO_x emission

Fig. 10 shows NO_x emission from the H_2 dual-fuel engine at 100% load and engine speed of 1500 rpm with and without water injection. It may be noted that NO_x emission increased significantly with the addition of H_2 due to high in-cylinder temperature, however, it decreased drastically with the addition of water along with H_2 fuel as the water reduces the in-cylinder temperature drastically. For 20% H_2 energy share, NO_x emission decreased from 8.67 g/kWh without water injection to 8.24, 6.62, and 5.47 g/kWh with SWC of 130, 200, and 270 g/kWh respectively. It decreased about 24% and 37% with SWC of 200 and 270 g/kWh in the H_2 dual-fuel engine at 20% H_2 energy share. It is well known that NO_x emission formation in CI engine is a strong function of in-cylinder temperature (Eqs. (14)–(19)), oxygen concentration and residence time. Water vapor in the combustion chamber leads to reduction in in-cylinder temperature and oxygen concentration which results in substantial reduction in NO_x emission.

Addition of water into the engine during the suction stroke could also increase the specific heat of the charge which leads to global temperature drop and further NO_x emission reduction. Ishida et al. obtained about 20% reduction in NO_x emission with the increase of 1% in specific heat of the gases in burned zone [34]. To maximize the emission reduction, water must be supplied into the flame area at the time of the emission formation. Supply of water before combustion starts (during the suction stroke itself) could reduce the emission formation during the first quarter of the combustion process (premixed combustion phase). As NO contributes a major portion of NO_x emission, the values of NO emission obtained from theoretical modeling are compared with the same scale of NO_x (Fig. 10). From the figure it is observed that the theoretical NO_x values are in agreement with the experimental results at an error ranging from 7% to 18%.

4.4. Effect of water injection on other emissions

The HC and CO emissions increased slightly with increasing SWC in the H_2 dual-fuel engine at rated load and speed (Fig. 11). As H_2 is carbon free energy carrier, its supplementation with B20 fuel decreases the emissions significantly [32]. The addition of H_2 fuel into the engine decreased all carbon based emissions drastically due to the high temperature combustion phenomenon; however the simultaneous addition of H_2 and water into the engine decreased the in-cylinder pressure/temperature (Fig. 4(b)) which lead to increase in these emissions. For 20% H_2 energy share, the HC emission increased from 0.008 g/kWh without water injection to 0.009, 0.013, and 0.016 g/kWh with SWC of 130, 200, and

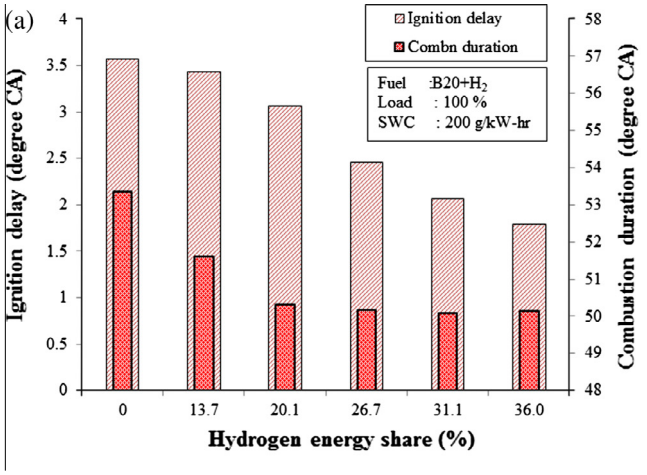

Fig. 5. Ignition delay and combustion duration variation.

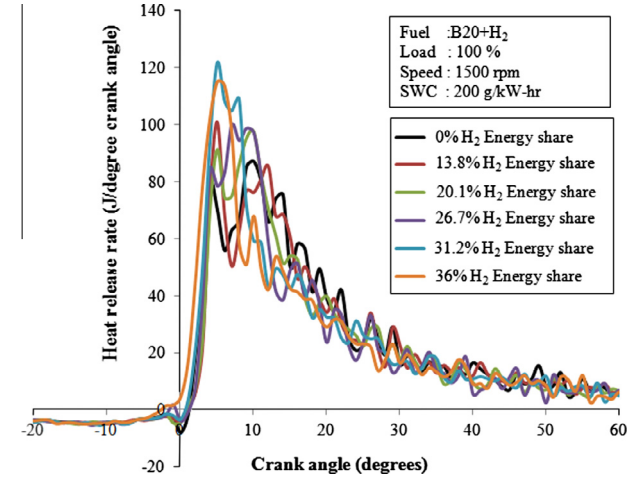

Fig. 6. Heat release rate profiles with respect to degree CA.

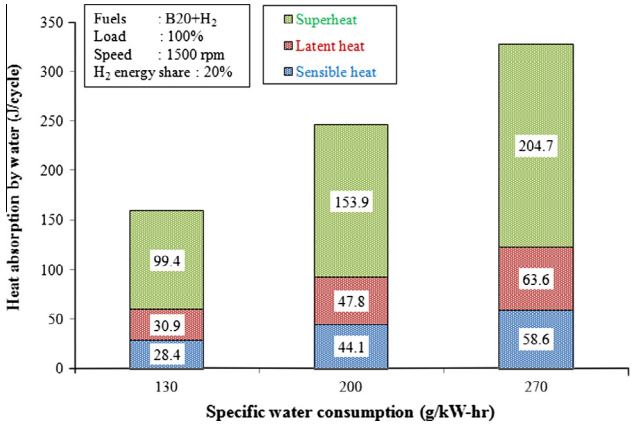

Fig. 7. Heat absorption with respect to water consumption.

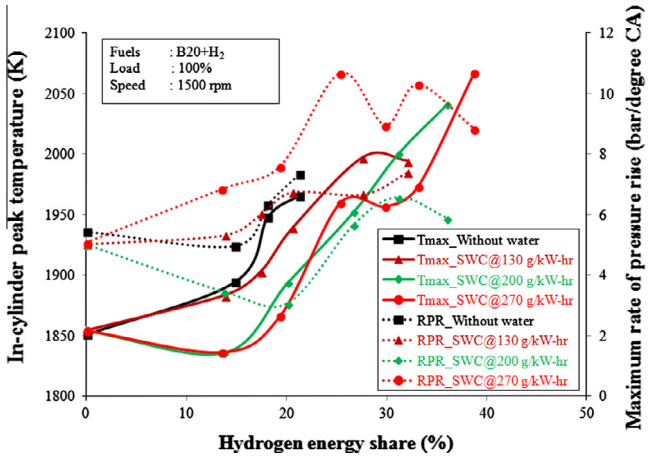

Fig. 8. In-cylinder peak temperature and maximum rate of pressure rise verses H_2 energy share.

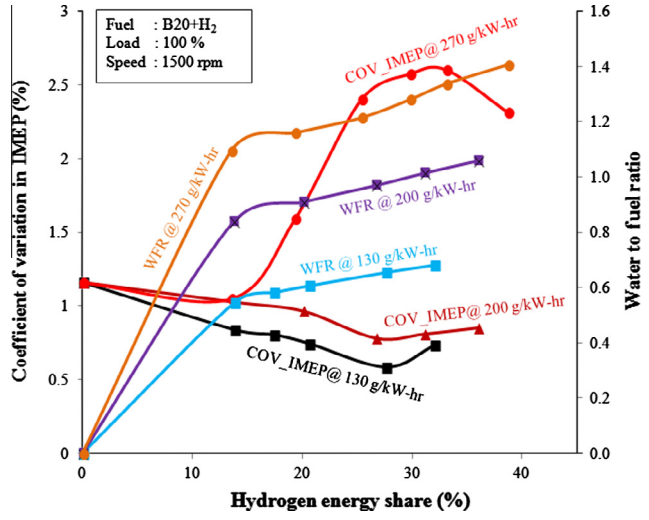

Fig. 9. COV in IMEP and water to fuel ratio variation with respect to H_2 energy share.

270 g/kWh respectively. Karim and Amoozegar reported that the water vapor in the chamber influences the compression stroke characteristics [35]. Vaporization of the water in the combustion chamber decreases the polytropic coefficient of compression stroke resulting in a drastic decrease of the temperature of the charge at the end of compression stroke. In addition, the water vapor affects badly on the pre-combustion processes such as vaporization of the pilot fuel, mixing of the pilot fuel with air, and pre-combustion chemical reactions due to which ignition delay period of the pilot fuel increases significantly as shown in Fig. 5(b). For a particular H_2 energy share, the ignition delay increased from 2.8°CA with SWC of 130 g/kWh to 3.7°CA with

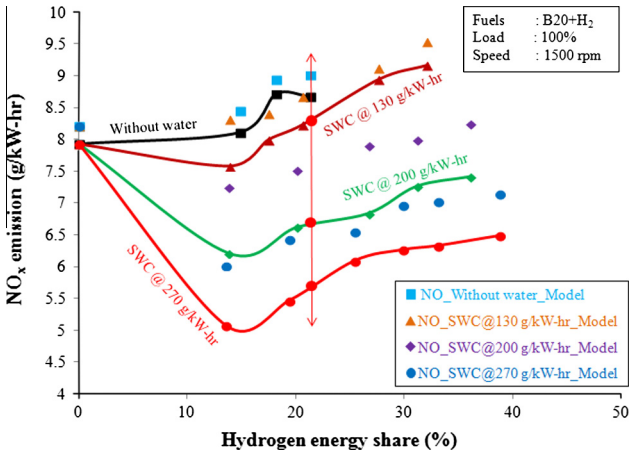

Fig. 10. NO_x emission verses H_2 energy share.

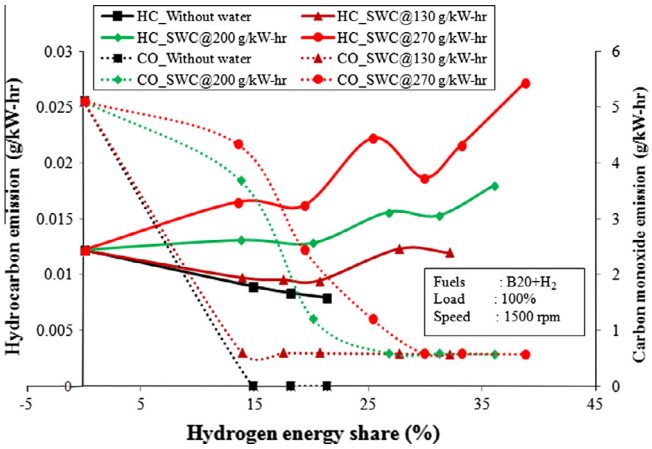

Fig. 11. Hydrocarbon and carbon monoxide emission verses H_2 energy share.

SWC of 270 g/kWh. This result is in an agreement with the earlier studies [19]. The water vapor in the combustion chamber also reduces the flame temperature and its speed during the early stage of combustion process [15]. With the low speed, the flame could not travel throughout the chamber, resulting in wall quenching of the flame. Enhancement of water quantity could further contribute to increase in quench layer thereby resulting in incomplete/partial combustion. Thus, the bulk quenching of the end charge at the combustion chamber walls causes significant increase in HC emissions.

It may also be noted that when the pilot fuel (B20) spray entrains the mixture of air + H_2 + water vapor instead of pure air, the chemical reaction rate could decrease due to a reduction in the temperature of the mixture. This decrease in combustion speed leads to partial oxidation of the air fuel charge and subsequently significant increase in CO emission. For 20% H_2 energy share, the emission increased from zero level without water injection to 0.595, 1.211, and 2.442 g/kWh with SWC of 130, 200, and 270 g/kWh respectively. Though the amount of the increased CO emission level is less, the percentage increase in the emission becomes 100% with water injected H_2 dual-fuel operation as compared to base H_2 dual-fuel operation at 20% H_2 energy share. Tauzia et al. also reported an increase in the CO emission from 22 g/h without water to 72 g/h with 5% water addition in a common rail direct injection diesel engine [19]. The CO emission formed during the hydrocarbon combustion mechanism is given by Eq. (39) [30]

$$RH \rightarrow R \rightarrow RO_2 \rightarrow RCHO \rightarrow RCO \rightarrow CO \quad (39)$$

The CO formed during the combustion via this route is then oxidized to CO_2 as given in Eq. (40). This reaction rate is dependent on the temperature exponentially as shown in Eq. (41). In case of water injection, this reaction rate decreases significantly due to a reduction in the combustion temperature, which promotes CO emission level. Tesfa et al. reported two main reasons for higher CO level with water injected diesel operation as compared to base diesel operation; (i) the reduction of pre-combustion temperature which slows down the chemical conversion of the CO to CO_2 and (ii) the solid carbon reaction with water vapor which enhances the formation of CO and H_2O in the combustion chamber [20].

$$CO + OH \rightarrow CO_2 + H \quad (40)$$

The rate constant for this reaction is

$$k_{f,CO} = 6.76 \times 10^{10} \exp(T/1102) \quad (41)$$

Smoke emission decreased drastically with increasing H_2 energy share under conventional H_2 dual-fuel operation as shown in Fig. 12. However, it increased considerably with water added H_2 dual-fuel operation due to heterogeneous combustion. It increased from 1.2% opacity without water injection to 2.7%, 3.9%, and 4.1% opacity with SWC of 130, 200, and 270 g/kWh respectively under dual-fuel mode (20% H_2 energy share) at rated load and speed (Fig. 12). Water vapor formed inside the cylinder chamber could affect the mixing process of fuel with air negatively, which leads to increase in degree of heterogeneity. Combustion with heterogeneous mixture is the one of the main reasons for the significant increase in smoke emission. Sarvi et al. also reported the similar trend of increase in particulate matter/smoke emission from 0.21 g/kWh without water injection to 0.28 g/kWh with a direct water injection at 75% load in a CI engine [21]. They stated the reasons for high smoke level that the temperature reduction at high loads while at low loads mixing of the gases during and after combustion. Tauzia et al. reported the reason for the high level of smoke emission that the reduction in the oxidation rate of smoke/soot/PM due to lower in-cylinder temperature [19]. Heywood reported the most of the PM resulted from incomplete combustion of hydrocarbon fuel [30]. Increased smoke/soot level deteriorates the lube oil performance also. Soot contaminated lube oil increases the friction between engine components so that it influences the engine performance badly [31]. This is also one of the major limiting aspect for addition of high amounts of water into the H_2 dual-fuel engine. Hence, a tradeoff needs to be done between NO_x and carbon based emissions such as HC, CO and smoke. In the present study, SWC of 200 g/kWh was selected as the optimum water quantity at the tradeoff condition for the emis-

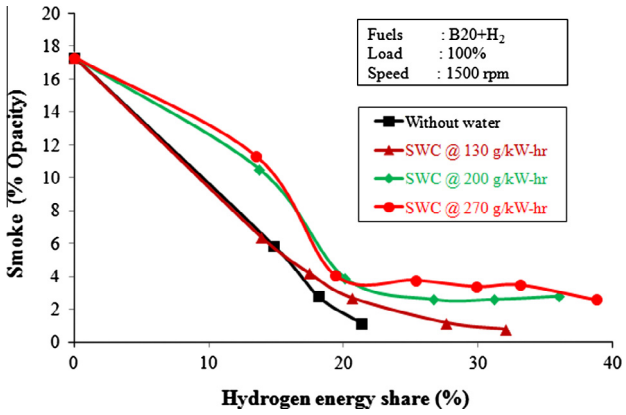

Fig. 12. Smoke emission verses H_2 energy share.

Table 4
Summary of effects of H_2/water addition on performance, combustion and emission characteristics of the test engine as compared to base diesel operation at 100% load.

S. No.	Description of the parameter	With increasing H_2 energy share	With increasing SWC
1	Energy efficiency	Increased	Decreased
2	HC emission	Decreased	Increased
3	CO emission	Decreased	Increased
4	Smoke emission	Decreased	Increased
5	NO_x emission	Increased	Decreased
6	In-cylinder pressure and peak pressure	Increased	Decreased
7	In-cylinder temperature and peak temperature	Increased	Decreased
8	Ignition delay	Decreased	Increased
9	Heat release rate	Increased	Decreased
10	Start of combustion	Advanced	Retarded
11	Combustion duration	Decreased	Increased

sions as well as energy efficiency. The summary of effect of H_2/water addition into the test engine on its performance and emission characteristics is given in Table 4.

5. Conclusions

The H_2 energy share improvement along with the NO_x emission reduction from a H_2 dual-fuel engine was studied using timed manifold water injection method. The following conclusions are drawn based on the experimental results;

- With base H_2 dual-fuel operation, the knock limited H_2 energy share was 20% without water injection at rated load and speed. The energy share increased to 32%, 36%, and 39% with SWC of 130, 200, and 270 g/kwh respectively for the same engine operating conditions.
- Degree of superheat of the water could be the major heat absorption source i.e., 63% of the total heat absorbed by the water among three kinds of heat energy.
- The SWC of 200 g/kWh with 36% H_2 energy share was selected as an optimum water quantity based on rate of pressure rise, COV in IMEP, better performance and lower emissions.
- Energy efficiency decreased slightly with water addition at rated load and speed, but it is still higher than the conventional CI engine.
- With water addition into the H_2 dual-fuel engine the in-cylinder peak pressure, peak temperature, and heat release rate decreased while ignition delay and combustion duration increased.
- A maximum of 37% reduction in NO_x emission could achieve with 270 g/kWh water addition with the penalty of a slight increase in carbon based emissions including HC, CO, and smoke.

However, these HC and CO emissions could easily be decreased with the utilization of oxidation catalysts in the tail pipe. A study on the effect of water added H_2 dual-fuel engine with the use of after treatment device on performance and emission characteristics of the engine needs to carried out in future for a complete solution.

Appendix A

Calculations for a set of conditions at rated load are given below;

$$\text{Brake power} = 7.4\ \text{kW}$$

$$\text{Mass flow rate of B20} = 0.328 \times 10^{-3}\ \text{kg/s}$$

$$\text{Mass flow rate of } H_2 = 0.0654 \times 10^{-3}\ \text{kg/s}$$

$$\text{Water flow rate} = 0.411 \times 10^{-3}\ \text{kg/s}$$

$$\text{Calorific value of B20} = 42.6\ \text{MJ/kg}$$

$$\text{Calorific value of } H_2 = 120\ \text{MJ/kg}$$

$$H_2\ \text{energy share} = \frac{0.0000654 \times 120{,}000}{(0.0000654 \times 120{,}000) + (0.000328 \times 42{,}600)} \times 100 = 36\%$$

$$\text{SWC} = \frac{0.000411 \times 60 \times 60}{7.4} \times 1000 = 200\ \text{g/kWh}$$

$$\text{Energy efficiency} = \frac{7.4}{(0.0000654 \times 120{,}000) + (0.000328 \times 42{,}600)} \times 100 = 34\%$$

References

[1] National Hydrogen Energy Road Map-2006 (Abridged Version, 2007). Path way for transition to hydrogen energy for India, National Hydrogen Energy Board, Ministry of New and Renewable Energy, Government of India; 2006. <http://mnre.gov.in/file-manager/UserFiles/abridged-nherm.pdf>. [Accessed 23.03.13].
[2] Babu MKG, Subramanian KA. Alternative transportation fuels: utilisation in combustion engines. New York: CRC Press; 2013.
[3] Bedoya ID, Saxena S, Cadavid FJ, Dibble RW, Wissink M. Experimental study of biogas combustion in an HCCI engine for power generation with high indicated efficiency and ultra-low NO_x emissions. Energy Convers Manage 2012;53:154–62.
[4] Swami Nathan S, Mallikarjuna JM, Ramesh A. An experimental study of the biogas–diesel HCCI mode of engine operation. Energy Convers Manage 2010;51:1347–53.
[5] Duc PM, Wattanavichien K. Study on biogas premixed charge diesel dual-fuelled engine. Energy Convers Manage 2007;48:2286–308.
[6] Makareviciene V, Sendzikiene E, Pukalskas S, Rimkus A, Vegneris R. Performance and emission characteristics of biogas used in diesel engine operation. Energy Convers Manage 2013;75:224–33.
[7] Ryu K. Effects of pilot injection pressure on the combustion and emissions characteristics in a diesel engine using biodiesel–CNG dual-fuel. Energy Convers Manage 2013;76:506–16.
[8] Saravanan N. An experimental investigation on manifold-injected hydrogen as a dual-fuel for diesel engine system with different injection duration. Int J Energy Res 2009;3:1352–66.
[9] Varde KS, Frame GA. Hydrogen aspiration in a direct injection type diesel engine-its effects on smoke and other engine performance parameters. Int J Hydrogen Energy 1983;8(7):549–55.
[10] Tsolakis A, Hernandez JJ, Megaritis A, Crampton M. Dual-fuel diesel engine operation using H_2: effect on particulate emissions. Energy Fuels 2005;19(2):418–25.
[11] Selim MYE. Sensitivity of dual-fuel engine combustion and knocking limits to gaseous fuel composition. Energy Convers Manage 2004;45:411–25.
[12] Carlucci AP, Laforgia D, Motz S, Saracino R, Wenzel SP. Advanced closed loop combustion control of a LTC diesel engine based on in-cylinder pressure signals. Energy Convers Manage 2014;77:193–207.
[13] Nande A, Wallner T, Naber J. Influence of water injection on performance and emissions of a direct-injection hydrogen research engine. SAE Paper 2008-01-2377; 2008.
[14] Palash SM, Masjuki HH, Kalam MA, Masum BM, Sanjid A, Abedin MJ. State of the art of NO_x mitigation technologies and their effect on the performance and emission characteristics of biodiesel-fuelled Compression Ignition engines. Energy Convers Manage 2013;76:400–20.
[15] Prabhukumar GP, Swaminathan S, Nagalingam B, Gopalakrishnan KV. Water induction studies in a hydrogen-diesel dual-fuel engine. Int J Hydrogen Energy 1987;12(3):177–86.
[16] Boretti A. Water injection in directly injected turbocharged spark ignition engines. Appl Therm Eng 2013;52:62–8.
[17] Mathur HB, Das LM, Patro TN. Hydrogen-fuelled diesel engine: performance improvement through charge dilution techniques. Int J Hydrogen Energy 1993;18(5):421–31.

[18] Subramanian KA. A comparison of water-diesel emulsion and timed injection of water into the intake manifold of a diesel engine for simultaneous control of NO and smoke emissions. Energy Convers Manage 2011;52:849–57.
[19] Tauzia X, Maiboom A, Shah SR. Experimental study of inlet manifold water injection on combustion and emissions of an automotive direct injection diesel engine. Energy 2010;35:3628–39.
[20] Tesfa B, Mishra R, Gu F, Ball AD. Water injection effects on the performance and emission characteristics of a CI engine operating with biodiesel. Renew Energy 2012;37:333–44.
[21] Sarvi A, Kilpinen P, Zevenhoven R. Emissions from large-scale medium-speed diesel engines: influence of direct water injection and common rail. Fuel Process Technol 2009;90:222–31.
[22] Adnan R, Masjuki HH, Mahlia TMI. Performance and emission analysis of hydrogen fuelled compression ignition engine with variable water injection timing. Energy 2012;43:416–26.
[23] Alahmer A. Influence of using emulsified diesel fuel on the performance and pollutants emitted from diesel engine. Energy Convers Manage 2013;73:361–9.
[24] Alahmer A, Yamin J, Sakhrieh A, Hamdan MA. Engine performance using emulsified diesel fuel. Energy Convers Manage 2010;51:1708–13.
[25] Liang Y, Shu G, Wei H, Zhang W. Effect of oxygen enriched combustion and water–diesel emulsion on the performance and emissions of turbocharged diesel engine. Energy Convers Manage 2013;73:69–77.
[26] Debnath BK, Sahoo N, Saha UK. Adjusting the operating characteristics to improve the performance of an emulsified palm oil methyl ester run diesel engine. Energy Convers Manage 2013;69:191–8.
[27] Gonca G. Investigation of the effects of steam injection on performance and NO emissions of a diesel engine running with ethanol–diesel blend. Energy Convers Manage 2014;77:450–7.
[28] Cesur I, Parlak A, Ayhan V, Boru B, Gonca G. The effects of electronic controlled steam injection on spark ignition engine. Appl Therm Eng 2013;55:61–8.
[29] Chintala V, Subramanian KA. A CFD (computational fluid dynamics) study for optimization of gas injector orientation for performance improvement of a dual-fuel diesel engine. Energy 2013;57:709–21.
[30] Heywood JB. Internal combustion engine fundamentals. McGraw-Hill Book Company; 1998.
[31] Chintala V, Subramanian KA. Assessment of maximum available work of a hydrogen fuelled compression ignition engine using exergy analysis. Energy 2014;67:162–75.
[32] Subramanian KA, Chintala V. Reduction of GHGs emissions in a biodiesel fuelled diesel engine using hydrogen. In: Proceedings of the ASME 2013 Internal Combustion Engine Fall Technical Conference (ICEF2013), October 13–16, 2013, Dearborn, Michigan. Paper No. ICEF2013-19133.
[33] Wagner W, Pruss A. International Equations for the Saturation properties of ordinary water substance. Revised according to the International Temperature Scale of 1990, Addendum to J. of Phys Chem Reference Data 1987; 16: 893.
[34] Ishida M, Hironoku U, Daisaku S. Prediction of NOx reduction to control exhaust emissions from heavy-duty diesel powered vehicles, SAE paper 972961; 1997.
[35] Karim GA, Amoozegar N. Examination of the performance of dual-fuel diesel engine with particular reference to the presence of some inert diluents in the engine intake charge, SAE Paper 821222; 1982.